IEEE Access
The journal for rapid open access publishing

Received October 8, 2015, accepted October 26, 2015, date of publication November 24, 2015,
date of current version December 10, 2015.

Digital Object Identifier 10.1109/ACCESS.2015.2503293

Radio Vortex–Multiple-Input Multiple-Output Communication Systems With High Capacity

QIBIAO ZHU[1,2], TAO JIANG[1], (Senior Member, IEEE), DAIMING QU[1], DA CHEN[1], AND NANRUN ZHOU[2]

[1]School of Electronics Information and Communications, Huazhong University of Science and Technology, Wuhan 430074, China
[2]School of Information Engineering, Nanchang University, Nanchang 330031, China

Corresponding author: T. Jiang (tao.jiang@ieee.org)

ABSTRACT As a potential technique to improve channel capacity, orbital angular momentum has been developed in the radio field. In this paper, a novel radio vortex–multiple-input multiple-output (RV-MIMO) system is proposed to provide high capacity in free space. In particular, the vortex channel of the proposed system is modeled. Based on this model, the optimal vortex phase is derived, which results in the optimal capacity of the proposed RV-MIMO system. Simulation results show that the proposed RV-MIMO system could achieve higher capacity than the MIMO system in free space.

INDEX TERMS Orbital angular momentum, radio vortex, multiple-input multiple-output, vortex phase.

I. INTRODUCTION

The fourth generation of mobile communication systems has rolled out across the globe, and the capacity demand is very significant for the emerging data services like ultra high definition videos and immersive multimedia [1]. In current wireless communications, capacity can be upgraded by using multiple-input multiple-output (MIMO) techniques. However, the existing MIMO systems have some issues in capacity increase. For example, the number of antennas is increased finitely. The employment of large-scale antenna arrays in the field of massive MIMO can bring substantial capacity improvements. However, the hardware impairment at each antenna should be considered [2]. Furthermore, for very large-scale antenna arrays, the capacity can be saturated to a certain level in the colored scattering environment [3]. In addition, propagation environment is increasingly severe. Therefore, capacity increase of the MIMO system becomes more difficult than before [4]. Even for the short-range line-of-sight (LOS) MIMO system in the three-dimensional (3D) space, the capacity is still limited by the transceiver distance, the wavelength and the array size [5]. Thus, capacity improvement of the MIMO systems is a crucial problem for wireless communication systems.

Recently, orbital angular momentum (OAM) has emerged as a promising technique to provide high capacity in the radio field. In 2011, the first experimental test of an OAM-based radio communication system was demonstrated. A radio signal and a radio signal with OAM of the system were transmitted and received on the same frequency simultaneously in a real world [6]. Then, OAM multiplexing was employed in millimetre-wave communications to provide high capacity [7]. From the viewpoint of the multiplexing, an OAM-based MIMO system can be regarded as a channel spatial multiplexing in the conventional MIMO systems [8]. Therefore, OAM multiplexing can be considered as a particular case of MIMO techniques, however, the multiplexing does not lead to any significant capacity improvement [9]. In other words, OAM-based radio communications do not bring any additional gains in capacity [10]. For an ideal OAM-based MIMO system, the transmission of radio signals with OAM could maximize channel capacity in the LOS scenario [11]. Since an OAM-based radio communication system can be modeled as the MIMO multiplexing system, the effective degrees of freedom in the OAM-based radio communication system depend on the characteristics of the circular array. The circular array is characterized by three parameters [12]. If the selection criteria is satisfied, multiple orthogonal sub-channels can be obtained in an ideal LOS OAM-based MIMO system which confirms to theories of conventional MIMO systems in spatial multiplexing [13]. In a word, the OAM-based MIMO system can be regarded as a conventional MIMO system since there is only an equivalent OAM mode at a certain time. When multiple OAM modes are coexisted in an ideal LOS scenario at any time, the channel of the OAM-base MIMO system should be considered. Furthermore, the relationship between the

IEEE Access
The journal for rapid open access publishing

vortex phase caused by the OAM and the capacity should be studied.

In this paper, a radio vortex–multiple-input multiple-output (RV-MIMO) system is proposed, where the vortex channel of the proposed system is modeled. Different from the MIMO systems, a radio signal with a vortex phase, is named as a vortex signal. A radio system with the vortex signal is called as a radio vortex (RV) system. Hence, the proposed system is combined with the RV and MIMO systems. The vortex phase of the proposed system brings an additional degree of freedom for capacity improvement. The vortex phase includes the azimuthal angle and the topological charge which is the eigenvalue of the vortex signal. The azimuthal angle depends on relative positions of the transmitting and receiving antennas, which are arranged into the uniform circular array (UCA), respectively. Therefore, variations of the relative rotation angle between the two UCAs could lead to different vortex phases due to different azimuthal angles. Moreover, the optimal vortex phase could be derived and the optimal capacity of the proposed RV-MIMO system is obtained. The basic idea of this paper is to exploit the vortex phase to achieve high capacity in the proposed RV-MIMO system. The key contributions are the modeling of the vortex channel and the derivation of the optimal vortex phase. Finally, simulation results validate the capacity improvement achieved by the proposed RV-MIMO system.

The rest of this paper is organized as follows. The RV-MIMO system model is introduced in Section II. Then the vortex channel of the proposed system is modeled in Section III. Based on this model, the optimal vortex phase is derived in Section IV. Simulations are conducted to verify the capacity increase of the proposed RV-MIMO system in Section V. Furthermore, the proposed system is compared with some related studies in Section VI. Finally, conclusions are drawn in Section VII.

II. SYSTEM MODEL

The proposed RV-MIMO system model is shown in Fig. 1. A pair of UCAs is employed at both transmitter and receiver. At the transmitter, data information is modulated to the millimetre-wave radio signals. The signals are then transmitted by collimated lensed-horn antennas and passed through spiral phase plates (SPPs) [7]. Note that, each transmitted antenna is matched to an SPP with different thicknesses to form different topological charges. Furthermore, the size of the SPP is larger than that of the lensed-horn antenna in order to limit possible effects that may arise from a truncated aperture. Therefore, the transmitted radio signals are modulated to the vortex signals due to the SPPs. At the receiver, multiple conventional antennas are arranged into the UCA to receive the vortex signals. The vortex signals could be demodulated to the radio signals by measuring the phase distribution with the phase interferometer [6] or other demodulation methods of the vortex signals. Then, the information could be recovered from the radio signals by the traditional demodulation method. The major notations in this paper are listed in Table 1.

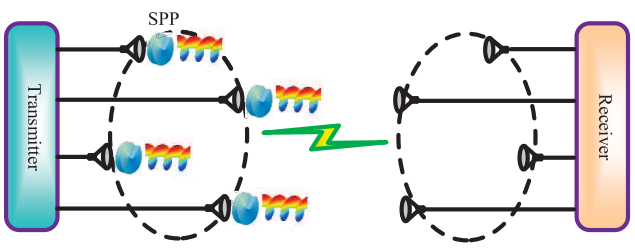

FIGURE 1. The proposed RV-MIMO system.

TABLE 1. Notations.

Notation	Definition
M	The number of receiving antennas
N	The number of transmitting antennas
$v(t, \varphi)$	The vortex signal at time t and the azimuthal angle φ
$s(t)$	The radio signal at time t
k	The topological charge
φ	The azimuthal angle
m	The m-th receiving antenna
n	The n-th transmitting antenna
φ_{mn}	The azimuthal angle from the n-th transmitting antenna to the m-th receiving antenna
$v_n(t, \varphi_{mn})$	The n-th vortex signal at time t and the azimuthal angle φ_{mn}
$y_m(t, \varphi_{mn})$	The m-th received signal at time t and the azimuthal angle φ_{mn}
$s_n(t)$	The n-th radio signal at time t
k_n	The topological charge of the n-th vortex signal
h_{mn}	The transfer function from the n-th transmitting antenna to the m-th receiving antenna
d_{mn}	The distance from the n-th transmitting antenna to the m-th receiving antenna
θ_{mn}	The rotation angle from the n-th transmitting antenna to the m-th receiving antenna
Θ	The relative rotation angle
R_{TX}	The radius of the UCA at the transmitter
R_{RX}	The radius of the UCA at the receiver
β	A constant contains attenuation and phase rotation
λ	Wavelength
C	The capacity of the MIMO system
C_{M}	The capacity of the 2×2 MIMO system
C_{MIMO}	The practical capacity of the MIMO system
C_{RM}	The capacity of the 2×2 RV-MIMO system
$C_{\mathrm{RM\text{-}Opt}}$	The optimal capacity of the 2×2 RV-MIMO system
$\mathbf{H}$	The $M \times N$ channel matrix
$\mathbf{H_v}$	The $M \times N$ vortex channel matrix
$\mathbf{H_{vn}}$	The $N \times N$ vortex channel matrix

Given that M receiving antennas and N transmitting antennas are configured, the proposed RV-MIMO system model could be extended from the MIMO model. A standard formulation of the input/output relationship in complex base-band notation is

$$\mathbf{y} = \mathbf{H_v}\mathbf{s} + \mathbf{w}, \tag{1}$$

where $\mathbf{y}$ is the received signal vector $\mathbf{y} = [y_1(t, \varphi_{1n}), y_2(t, \varphi_{2n}), \ldots, y_m(t, \varphi_{mn}), \ldots, y_M(t, \varphi_{Mn})]^T$, and $[\cdot]^T$ denotes transposition. Analogously, $\mathbf{s}$ is the transmitted radio

signal vector $\mathbf{s} = [s_1(t), s_2(t), \ldots, s_n(t), \ldots, s_N(t)]^T$, and $\mathbf{w}$ is the additive white Gaussian noise (AWGN) vector $\mathbf{w} = [w_1(t), w_2(t), \ldots, w_m(t), \ldots, w_M(t)]^T$. All the elements are independent and identically distributed (i. i. d.) zero mean complex Gaussian random variables with unity variance. Specially, $\mathbf{H_v}$ is the $M \times N$ vortex channel matrix.

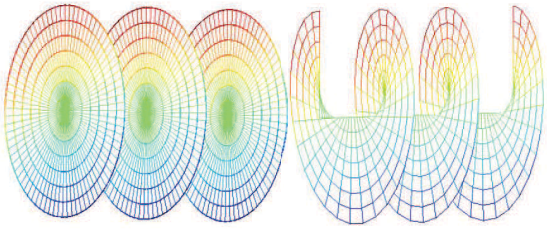

FIGURE 2. Different phase fronts of a radio signal and a vortex signal. (a) Radio signal. (b) Vortex signal.

III. VORTEX CHANNEL

As demonstrated in Fig. 2, the radio signal has planar phase fronts. However, the mentioned vortex signal in the proposed RV-MIMO system has a helical phase front. For implementation, the helical phase front can be yielded by the SPP [7]. Theoretically, the vortex signal can be formed by multiplying an $e^{jk\varphi}$ term to a radio signal in order to achieve the helical phase front. Thus, the vortex signal can be modeled as

$$v(t, \varphi) = s(t)e^{jk\varphi}, \tag{2}$$

where $s(t)$ is the radio signal, k denotes the topological charge, and φ is the azimuthal angle. When the transmitted radio signal is passed through the SPP, the vortex signal is generated with a topological charge. Given that the n-th radio signal is expressed as $s_n(t)$, the corresponding n-th vortex signal could be expressed as

$$v_n(t, \varphi_{mn}) = s_n(t)e^{jk_n\varphi_{mn}}, \tag{3}$$

where k_n is the topological charge of the n-th vortex signal, and φ_{mn} is the azimuthal angle from the n-th transmitting antenna to the m-th receiving antenna in Fig.3. T_n is the n-th transmitting antenna, while R_m is the m-th receiving antenna. T'_n and R'_m are the geometric projections of T_n and R_m, respectively.

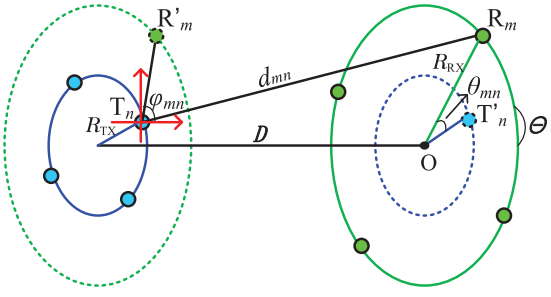

FIGURE 3. Two UCAs are at the transmitter and the receiver, respectively.

Suppose that the MIMO channel matrix is $\mathbf{H}$, let $\mathbf{H}$ be an $M \times N$ matrix as

$$\mathbf{H} = \begin{bmatrix} h_{11} & h_{12} & \cdots & h_{1N} \\ h_{21} & h_{22} & \cdots & h_{2N} \\ \vdots & \vdots & h_{mn} & \vdots \\ h_{M1} & h_{M2} & \cdots & h_{MN} \end{bmatrix}, \tag{4}$$

where h_{mn} is the transfer function from the n-th transmitting antenna to the m-th receiving antenna. Note that, a free-space link has been employed in the current studies for the propagation of the vortex signals [6], [7], [10] since the singularity should be calibrated between the transmitter and the receiver [6]. Hence, the proposed RV-MIMO system is also applied to the free-space scenario. According to [10], h_{mn} is given by

$$h_{mn} = \beta \frac{\lambda}{4\pi d_{mn}} e^{-j2\pi \frac{d_{mn}}{\lambda}}, \tag{5}$$

where β is a constant, which contains attenuation and phase rotation, λ denotes wavelength, and d_{mn} is the distance from the n-th transmitting antenna to the m-th receiving antenna. Thus,

$$\mathbf{H} = \frac{\beta\lambda}{4\pi} \begin{bmatrix} \frac{e^{-j2\pi \frac{d_{11}}{\lambda}}}{d_{11}} & \frac{e^{-j2\pi \frac{d_{12}}{\lambda}}}{d_{12}} & \cdots & \frac{e^{-j2\pi \frac{d_{1N}}{\lambda}}}{d_{1N}} \\ \frac{e^{-j2\pi \frac{d_{21}}{\lambda}}}{d_{21}} & \frac{e^{-j2\pi \frac{d_{22}}{\lambda}}}{d_{22}} & \cdots & \frac{e^{-j2\pi \frac{d_{2N}}{\lambda}}}{d_{2N}} \\ \vdots & \vdots & \ddots & \vdots \\ \frac{e^{-j2\pi \frac{d_{M1}}{\lambda}}}{d_{M1}} & \frac{e^{-j2\pi \frac{d_{M2}}{\lambda}}}{d_{M2}} & \cdots & \frac{e^{-j2\pi \frac{d_{MN}}{\lambda}}}{d_{MN}} \end{bmatrix}. \tag{6}$$

For the RV-MIMO system, when the vortex signal vectors are denoted as $\mathbf{v} = [v_1(t, \varphi_{m1}), v_2(t, \varphi_{m2}), \ldots, v_n(t, \varphi_{mn}), \ldots, v_N(t, \varphi_{mN})]^T$, the m-th received signal $y_m(t)$ could be described as

$$\begin{aligned} y_m(t, \varphi_{mn}) &= \sum_{n=1}^{N} h_{mn} v_n(t, \varphi_{mn}) + w_m(t) \\ &= \sum_{n=1}^{N} h_{mn} s_n(t) e^{jk_n\varphi_{mn}} + w_m(t). \end{aligned} \tag{7}$$

Therefore, the received signal vector is

$$\begin{aligned} \mathbf{y} &= \mathbf{H}\mathbf{v} + \mathbf{w} \\ &= \mathbf{H} \odot \begin{bmatrix} e^{jk_1\varphi_{11}} & e^{jk_2\varphi_{12}} & \cdots & e^{jk_N\varphi_{1N}} \\ e^{jk_1\varphi_{21}} & e^{jk_2\varphi_{22}} & \cdots & e^{jk_N\varphi_{2N}} \\ \vdots & \vdots & e^{jk_m\varphi_{mn}} & \vdots \\ e^{jk_1\varphi_{M1}} & e^{jk_2\varphi_{M2}} & \cdots & e^{jk_N\varphi_{MN}} \end{bmatrix} \mathbf{s} + \mathbf{w}. \end{aligned} \tag{8}$$

According to (1), the vortex channel matrix could be derived as

$$\mathbf{H_v} = \frac{\beta\lambda}{4\pi}\begin{bmatrix} \frac{e^{jk_1\varphi_{11}-j2\pi\frac{d_{11}}{\lambda}}}{d_{11}} & \cdots & \frac{e^{jk_N\varphi_{1N}-j2\pi\frac{d_{1N}}{\lambda}}}{d_{1N}} \\ \frac{e^{jk_1\varphi_{21}-j2\pi\frac{d_{21}}{\lambda}}}{d_{21}} & \cdots & \frac{e^{jk_N\varphi_{2N}-j2\pi\frac{d_{2N}}{\lambda}}}{d_{2N}} \\ \vdots & \ddots & \vdots \\ \frac{e^{jk_1\varphi_{M1}-j2\pi\frac{d_{M1}}{\lambda}}}{d_{M1}} & \cdots & \frac{e^{jk_N\varphi_{MN}-j2\pi\frac{d_{MN}}{\lambda}}}{d_{MN}} \end{bmatrix}. \quad (9)$$

Compared with the MIMO channel $\mathbf{H}$, the vortex channel $\mathbf{H_v}$ of the RV-MIMO system can be considered as the MIMO channel with vortex phase terms. The vortex phase of the proposed RV-MIMO system includes the azimuthal angle and the topological charge which is the eigenvalue of the vortex signal. The azimuthal angle depends on relative positions of the transmitting and receiving antennas, which are arranged into the UCAs, respectively.

Two UCAs are shown in Fig.3. The two UCAs are placed in parallel, and they face each other on the same beam axis at a distance D. R_{TX} and R_{RX} are radii of the two UCAs at the transmitter and receiver, respectively. Θ is the relative rotation angle of the two UCAs. The UCA at the transmitter is fixed. However, the UCA at the receiver is active. In other words, the relative rotation angle Θ is variable. Specifically, two cases are considered for the UCA at the receiver. Firstly, the central point O is fixed and the relative rotation angle Θ of the two UCAs is variable. Therefore, the two central points of the two UCAs coincide. Secondly, both the central point O and the relative rotation angle Θ are variable. The dots on the two concentric circles indicate the positions of the antenna elements. The dashed line denotes the geometrical projection due to illustration of the azimuthal angle φ_{mn} and the rotation angle θ_{mn}.

For the first case, when the central point O of the UCA at the receiver is fixed, the distance d_{mn} between arbitrary two transmitting and receiving antennas is calculated as

$$d_{mn} = (D^2 + R_{\mathrm{TX}}^2 + R_{\mathrm{RX}}^2 - 2R_{\mathrm{TX}}R_{\mathrm{RX}}\cos\theta_{mn})^{\frac{1}{2}}. \quad (10)$$

The rotation angle θ_{mn} between arbitrary two transmitting and receiving antennas is written as

$$\theta_{mn} = 2\pi\left(\frac{m}{M} - \frac{n}{N}\right) + \Theta, \quad (11)$$

where m and n are the m-th receiving antenna and the n-th transmitting antenna, respectively. For the proposed RV-MIMO system, assume that the locations of antennas are known, then the azimuthal angle φ_{mn} is expressed as

$$\varphi_{mn} = \mathrm{Angle}\left\{R_{\mathrm{RX}}\cos\left(2\pi\frac{m}{M} + \Theta\right) - R_{\mathrm{TX}}\cos\left(2\pi\frac{n}{N}\right) + j\left[R_{\mathrm{RX}}\sin\left(2\pi\frac{m}{M} + \Theta\right) - R_{\mathrm{TX}}\sin\left(2\pi\frac{n}{N}\right)\right]\right\}, \quad (12)$$

where the Angle$(\cdot)$ denotes the achieving azimuthal angle operation.

Different from the first case, the central point O of the UCA at the receiver is not fixed in the second case, and the central point is assumed to move from the origin position (0, 0) to the new position $(x_{\mathrm{c}}, y_{\mathrm{c}})$. According to the geometry, d_{mn} is denoted as

$$d_{mn} = \left\{D^2 + \left[x_{\mathrm{c}} + R_{\mathrm{RX}}\cos\left(2\pi\frac{m}{M} + \Theta\right) - R_{\mathrm{TX}}\cos\left(2\pi\frac{n}{N}\right)\right]^2 + \left[y_{\mathrm{c}} + R_{\mathrm{RX}}\sin\left(2\pi\frac{m}{M} + \Theta\right) - R_{\mathrm{TX}}\sin\left(2\pi\frac{n}{N}\right)\right]^2\right\}^{\frac{1}{2}}. \quad (13)$$

In addition, the azimuthal angle φ_{mn} can be expressed as

$$\varphi_{mn} = \mathrm{Angle}\{x_{\mathrm{c}} + R_{\mathrm{RX}}\cos(2\pi\frac{m}{M} + \Theta) - R_{\mathrm{TX}}\cos(2\pi\frac{n}{N}) + j\,[y_{\mathrm{c}} + R_{\mathrm{RX}}\sin(2\pi\frac{m}{M} + \Theta) - R_{\mathrm{TX}}\sin(2\pi\frac{n}{N}]\}. \quad (14)$$

Hitherto, the vortex channel matrix $\mathbf{H_v}$ could be obtained since the distance d_{mn} and the azimuthal angle φ_{mn} are achieved. Note that, λ is a constant wavelength of the radio signals. In addition, the topological charges $k_1, k_2, \ldots, k_n$ are constants determined by the SPP.

In summary, when the relative rotation angles of the two UCAs are variable, two cases should be considered to the vortex channel at the receiver: the fixed UCA and the movable UCA. Moreover, the optimal vortex phase of the vortex channel in the proposed RV-MIMO system should be derived.

IV. THE OPTIMAL VORTEX PHASE FOR CAPACITY

The variation of the relative rotation angles affects the azimuthal angle φ_{mn} and further affects the vortex phase and the vortex channel matrix $\mathbf{H_v}$. According to the Shannon's channel capacity theorem, the vortex channel matrix impacts on the capacity of the proposed RV-MIMO system. Moreover, the vortex phase is the main characteristic of the vortex signal. The vortex signal of the RV-MIMO system is orthogonal and independent in the time and the frequency domains since the vortex phase of the proposed system is an additional degree of freedom. Thus, there will be no impact on current communication systems if the RV-MIMO system is deployed in the future.

Suppose that the transmitter does not know the channel state information (CSI), the transmitter cannot optimize its power allocation. Thus, the best strategy would allocate equal power to each transmitting antenna. Under this assumption, according to the Shannon's channel capacity theorem, the capacity of the MIMO system is given by

$$C = \log_2\left[\det\left(\mathbf{I} + \frac{\mathrm{SNR}}{N}\mathbf{H}\mathbf{H}^H\right)\right] \text{ bps/Hz}, \quad (15)$$

where det $(\cdot)$ denotes the determinant, $\mathbf{I}$ is the identity matrix with the size given by a minimum number of transmitting antennas (N) and receiving antennas (M), SNR is the signal-to-noise ratio, and $\mathbf{H}$ represents the $M \times N$ channel

matrix with the $\mathbf{H}^H$ denoting the conjugate transpose. For the 2 × 2 MIMO system, the capacity is

$$C_{\mathrm{M}} = \log_2 \left\{ 1 + \frac{\mathrm{SNR}}{2} \sum_{m=1}^{2} \sum_{n=1}^{2} |h_{mn}|^2 + \left(\frac{\mathrm{SNR}}{2}\right)^2 (|h_{11}|^2|h_{22}|^2 + |h_{12}|^2|h_{21}|^2) - 2\left(\frac{\beta\lambda}{4\pi}\right)^4 \frac{1}{d_{11}d_{12}d_{21}d_{22}} \cos\gamma \right\}, \quad (16)$$

where,

$$\gamma = \frac{2\pi}{\lambda}(d_{11} - d_{12} - d_{21} + d_{22}). \quad (17)$$

According to (13) and (14), suppose that $\Theta = 0$,

$$\gamma = \frac{4\pi D}{\lambda} \left[\sqrt{1 + \left(\frac{R_{\mathrm{TX}} - R_{\mathrm{RX}}}{D}\right)^2} - \sqrt{1 + \left(\frac{R_{\mathrm{TX}} + R_{\mathrm{RX}}}{D}\right)^2} \right]. \quad (18)$$

Generally speaking, D is far larger than R_{TX} and R_{RX} in practical radio communications. Therefore, $\gamma \approx 0$ results in $\cos\gamma = 1$. As a result, the practical capacity of the MIMO system is

$$C_{\mathrm{MIMO}} = \log_2 \left\{ 1 + \frac{\mathrm{SNR}}{2} \sum_{m=1}^{2} \sum_{n=1}^{2} |h_{mn}|^2 + \left(\frac{\mathrm{SNR}}{2}\right)^2 (|h_{11}|^2|h_{22}|^2 + |h_{12}|^2|h_{21}|^2) - 2\left(\frac{\beta\lambda}{4\pi}\right)^4 \frac{1}{d_{11}d_{12}d_{21}d_{22}} \right\}. \quad (19)$$

However, the practical capacity of the RV-MIMO system depends on the vortex phase associated with the relative positions. Varying relative positions of the UCA at the receiver in a certain range to find the optimal vortex phase is a feasible way to achieve the optimal capacity.

A. THE OPTIMAL VORTEX PHASE OF THE 2 × 2 RV-MIMO SYSTEM

For the 2 × 2 RV-MIMO system in Fig. 4, T_1 and T_2 are the transmitting antennas, while R_1 and R_2 are the receiving antennas. When $\mathbf{H}_{\mathbf{v}}$ is applied to (15), the capacity of the 2 × 2 RV-MIMO system is expressed as (20), shown at the bottom of this page, where,

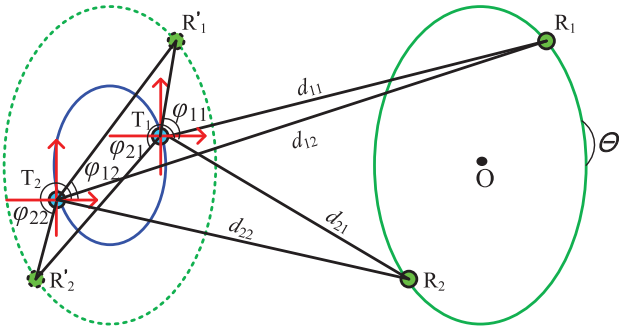

FIGURE 4. Distances and azimuthal angles of the 2 × 2 RV-MIMO system.

$$A = 2\left(\frac{\beta\lambda}{4\pi}\right)^4 \frac{1}{d_{11}d_{12}d_{21}d_{22}} \cos(B - C). \quad (21)$$

Note that, B is the vortex phase, and C denotes the phase of the MIMO system.

$$B = k_1(\varphi_{11} - \varphi_{21}) + k_2(\varphi_{22} - \varphi_{12}),$$
$$C = 2\pi \frac{d_{11} - d_{12} - d_{21} + d_{22}}{\lambda}. \quad (22)$$

Therefore, varying the relative rotation angle Θ, even changing the central point of the UCA at the receiver could achieve different azimuthal angles φ_{mn}. Furthermore, different thicknesses of the SPP are selected for different topological charges. Thus, the optimal vortex phase is attained and leads to the optimal capacity of the RV-MIMO system. The optimal capacity of the 2 × 2 RV-MIMO system could be achieved as

$$C_{\mathrm{RM\text{-}Opt}} = \log_2 \left\{ 1 + \frac{\mathrm{SNR}}{2} \sum_{m=1}^{2} \sum_{n=1}^{2} |h_{mn}|^2 + \left(\frac{\mathrm{SNR}}{2}\right)^2 (|h_{11}|^2|h_{22}|^2 + |h_{12}|^2|h_{21}|^2) + 2\left(\frac{\beta\lambda}{4\pi}\right)^4 \frac{1}{d_{11}d_{12}d_{21}d_{22}} \right\}. \quad (23)$$

Correspondingly, the optimal vortex phase of the 2 × 2 RV-MIMO system should satisfy the following condition:

$$B - C = (2a + 1)\pi, \quad a = 0, \pm 1, \pm 2, \ldots \quad (24)$$

$$\begin{aligned} C_{\mathrm{RM}} &= \log_2 \det(\mathbf{I}_2 + \frac{\mathrm{SNR}}{2}\mathbf{H}_{\mathbf{v}}\mathbf{H}_{\mathbf{v}}^H) \\ &= \log_2 \begin{vmatrix} 1 + \frac{\mathrm{SNR}}{2} \sum_{n=1}^{2} h_{1n}h_{1n}^* & \frac{\mathrm{SNR}}{2} \sum_{n=1}^{2} h_{1n}h_{2n}^* e^{jk_n(\varphi_{1n} - \varphi_{2n})} \\ \frac{\mathrm{SNR}}{2} \sum_{n=1}^{2} h_{2n}h_{2n}^* e^{jk_n(\varphi_{2n} - \varphi_{1n})} & 1 + \frac{\mathrm{SNR}}{2} \sum_{n=1}^{2} h_{2n}h_{2n}^* \end{vmatrix} \\ &= \log_2 \left\{ 1 + \frac{\mathrm{SNR}}{2} \sum_{m=1}^{2} \sum_{n=1}^{2} |h_{mn}|^2 + \left(\frac{\mathrm{SNR}}{2}\right)^2 (|h_{11}|^2|h_{22}|^2 + |h_{12}|^2|h_{21}|^2 - A) \right\} \end{aligned} \quad (20)$$

In summary, the optimal capacity of the 2 × 2 RV-MIMO system could be attained when the optimal vortex phase is satisfied (24).

B. THE OPTIMAL VORTEX PHASE OF THE N × N RV-MIMO SYSTEM

To simplify the analysis for the $N \times N$ RV-MIMO system, the amplitude of the vortex channel could be normalized to unity. We have,

$$\mathbf{H_{vn}} = \begin{bmatrix} e^{jk_1\varphi_{11}-j2\pi\frac{d_{11}}{\lambda}} & \cdots & e^{jk_N\varphi_{1N}-j2\pi\frac{d_{1N}}{\lambda}} \\ e^{jk_1\varphi_{21}-j2\pi\frac{d_{21}}{\lambda}} & \cdots & e^{jk_N\varphi_{2N}-j2\pi\frac{d_{2N}}{\lambda}} \\ \vdots & \ddots & \vdots \\ e^{jk_1\varphi_{M1}-j2\pi\frac{d_{M1}}{\lambda}} & \cdots & e^{jk_N\varphi_{MN}-j2\pi\frac{d_{MN}}{\lambda}} \end{bmatrix}. \quad (25)$$

Based on this idea, the derivation is repeated as the optimal vortex phase of the 2 × 2 RV-MIMO system. The optimal vortex phase of the $N \times N$ RV-MIMO system should satisfy the following condition:

$$\begin{aligned} &\{k_n^*, \varphi_{mn}^*, d_{mn}^*\} \\ &= \arg\max_{\mathbf{H_{vn}}:\mathrm{T_r}[\mathbf{H_{vn}}]\le P} \log_2 \det\left(\mathbf{I}_N + \frac{\mathrm{SNR}}{N}\mathbf{H_{vn}}\mathbf{H_{vn}}^H\right) \\ &= \arg\min_{k_n,\varphi_{mn},d_{mn}} \prod_{m=1}^{N}\prod_{n=1}^{N} 2\cos\left[\sum_{m=1}^{N}\sum_{n=1}^{N}(-1)^{m+n} \right. \\ &\qquad \left. \times\left(k_n\varphi_{mn} - 2\pi\frac{d_{mn}}{\lambda}\right)\right], \end{aligned} \quad (26)$$

where P is the total power. Obviously, the optimal condition could be expressed as

$$\begin{aligned} &\sum_{m=1}^{N}\sum_{n=1}^{N}(-1)^{m+n}\left(k_n\varphi_{mn} - 2\pi\frac{d_{mn}}{\lambda}\right) \\ &\quad = (2a+1)\pi, \quad a = 0, \pm1, \pm2, \ldots \end{aligned} \quad (27)$$

In summary, the optimal capacity of the $N \times N$ RV-MIMO system could be achieved when the amplitude of the $N \times N$ RV-MIMO system is normalized and the vortex phase satisfies the condition (27).

V. SIMULATION RESULTS

In this paper, both the proposed RV-MIMO and the MIMO systems are discussed in free space. The main parameters of the RV-MIMO and the MIMO systems are listed in Table 2. The radii of the UCAs at the transmitter and receiver are R_{TX} and R_{RX}, respectively. In addition, the total powers of the two systems are the same, and each transmitting antenna is assigned power equally. Note that, when a transmitted radio signal is passed through an SPP, a vortex signal is generated. Each vortex signal carries a topological charge k_n which is from 0 to $N-1$. The number of topological charges has no relationship with the power.

TABLE 2. Parameters of the RV-MIMO system.

Parameter	Value
λ	$0.01m$
R_{TX}	0.6λ
R_{RX}	0.8λ
D	7000λ
Θ	$0 \sim 2\pi$

In the following configurations, the UCA at the transmitter is fixed. Nevertheless, there are two cases about the central point of the UCA at the receiver to be considered: One is fixed, the other is movable in a certain range. For both of the two cases, the relative rotation angles Θ are varied from 0 to 2π in order to find the optimal vortex phase for the optimal capacity of the RV-MIMO system. The optimal capacity of the RV-MIMO system is labeled as "Optimal" in the simulation results. Note that, the capacities of the RV-MIMO system and the MIMO system are defined as the average capacity for the variations of the relative rotation angles. In addition, the capacity gain is defined as the optimal capacity of the RV-MIMO system to the capacity of the MIMO system with the identical SNR.

A. THE FIXED UCA AT THE RECEIVER

In this case, the central points of the two UCAs are coincided. As shown in Fig. 5, for the 2 × 2 RV-MIMO system and the 2 × 2 MIMO system, three types of capacities are illustrated with the Monte Carlo method. In addition, the optimal capacity of the RV-MIMO system in theory is demonstrated under the condition of the optimal vortex phase (24). Obviously, it is consistent with the Monte Carlo result. Therefore, in the next simulations, we could employ the Monte Carlo method to replace the theoretical method to achieve the optimal capacity avoiding complicate derivations for two more antennas. The optimal capacity is a little higher than the capacity of the RV-MIMO system with the identical SNR since the optimal vortex phase is employed. For example, the optimal capacity and the capacity of the RV-MIMO system are 13.32 bps/Hz and 12.93 bps/Hz at SNR=20 dB, respectively. Furthermore, the capacity of the RV-MIMO system is higher than that of the MIMO system with identical

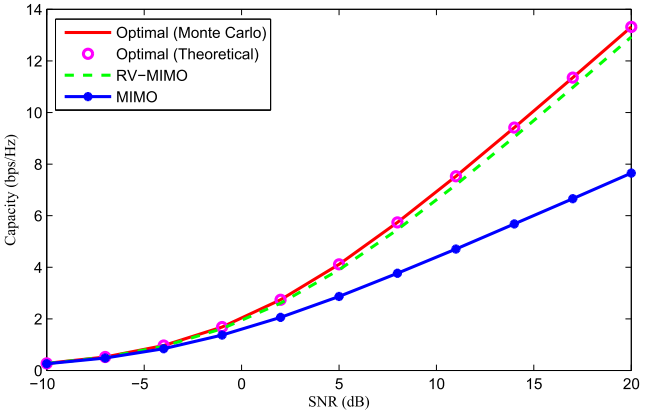

FIGURE 5. Capacities of the 2 × 2 RV-MIMO system and the 2 × 2 MIMO system.

SNR since the vortex phase is exploited. For instance, the capacities of the RV-MIMO system and the MIMO system are 12.93 bps/Hz and 7.65 bps/Hz at SNR=20 dB, respectively. Thus, with the increase of SNRs, the capacity improvement of the RV-MIMO system is more significant than that of its counterpart due to the contribution of the vortex phase.

Different types of the capacities are demonstrated in Fig. 6. The capacities of both the RV-MIMO and MIMO systems are enhanced when SNR increases.

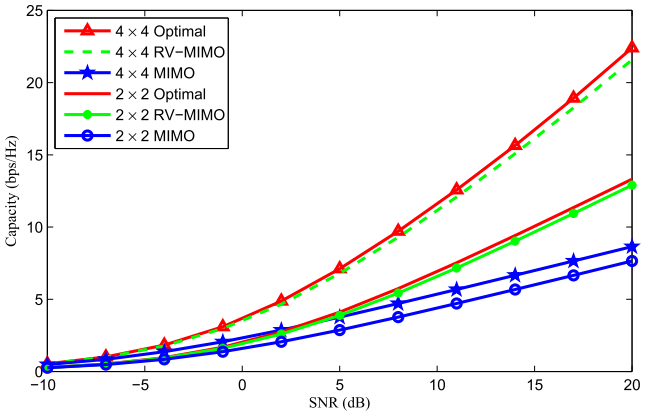

FIGURE 6. Comparisons between the RV-MIMO system and the MIMO system.

For the identical number of antennas, the capacities of the RV-MIMO system are higher than those of the MIMO system under the same SNR due to the vortex phase. For example, when SNR is 20 dB, the capacities of the 4 × 4 RV-MIMO system and the 4 × 4 MIMO system are 21.57 and 8.648 bps/Hz, respectively. Furthermore, the optimal capacity is 22.4 bps/Hz at SNR=20 dB. Compared with the capacity of the MIMO system at SNR=20 dB, the optimal capacity and the capacity of the RV-MIMO system are increased by 13.752 and 12.922 bps/Hz, respectively.

For the identical types of capacities, the capacity improvement of the RV-MIMO system is more significant than that of its counterpart with the increase of SNRs. For the MIMO system, it could not obtain the obvious capacity improvement although SNR is increased. For example, when SNR is 20 dB, the capacities of the 4 × 4 MIMO system and the 2 × 2 MIMO system are 8.648 and 7.651 bps/Hz, respectively. Therefore, the capacity is improved 1.13 times at SNR=20 dB. With the same SNR to the RV-MIMO system, the capacities of the 4 × 4 RV-MIMO system and the 2 × 2 RV-MIMO system are 21.57 and 12.9 bps/Hz, respectively. Hence, the capacity of the RV-MIMO is improved 1.67 times at SNR=20 dB. Analogously, the optimal capacity is increased 1.68 times at SNR=20 dB. Thus, the optimal capacity is promoted higher than both the capacities of the RV-MIMO and the MIMO systems in the identical situation.

Fig. 7 shows the relationship between the capacity gain and SNR. For the identical number of antennas, the gains are advanced with the increase of SNRs. For example, the gains of the 4 × 4 RV-MIMO system are 1.113 at SNR=−10 dB

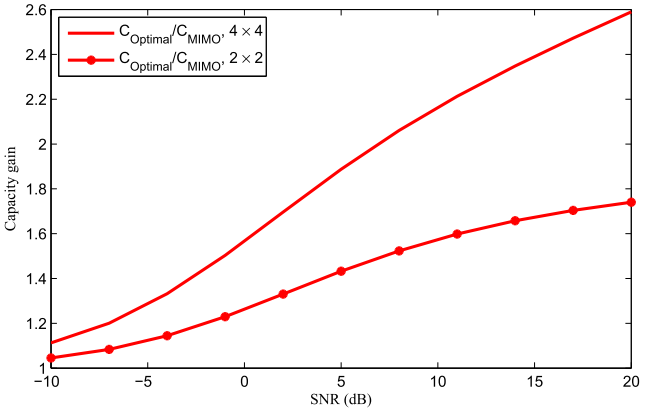

FIGURE 7. Capacity gains of the RV-MIMO system over the MIMO system.

and 2.59 at SNR=20 dB, respectively. The capacity gain is about 2.33 times increased for the 4 × 4 RV-MIMO system. Therefore, the improvement of the capacity gains is significant with the increase of SNRs. For the identical SNRs, the more antennas, the better benefits. For instance, when SNR is 20 dB, the gains of the 4 × 4 RV-MIMO system and the 2 × 2 RV-MIMO system are 2.59 and 1.74, respectively. The capacity gain is improved about 1.49 times at SNR=20 dB. Therefore, the capacity gains of the RV-MIMO system are increased with increasing antennas.

In conclusion, with the increase of the antennas and SNRs, the capacity of the RV-MIMO system is more remarkable than that of the MIMO system since the optimal vortex phase is exploited.

B. THE MOVABLE UCA AT THE RECEIVER

In this case, the central point of the UCA at the receiver is active within an alignment range, and SNR is 8 dB. Based on this scenario, the relative rotation angle is still varying from 0 to 2π to find the optimal vortex phase.

As illustrated in Fig. 8, different numbers of antennas are considered in the relationship between the alignment range and the capacity. For the MIMO system, the capacities of the

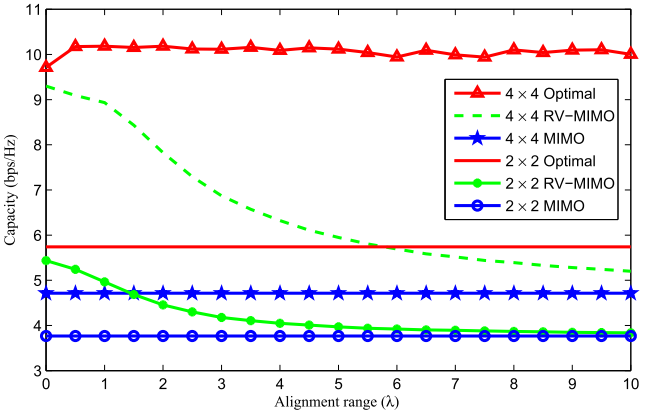

FIGURE 8. The relationship between the capacity and the alignment range.

2×2 and 4×4 MIMO systems keep fixed values: 3.768 bps/Hz and 4.714 bps/Hz, respectively. The capacities are not variable when the alignment range from 0 to 10λ since the MIMO systems have no vortex phases, and the capacities of the MIMO systems have no relationship with the alignment range.

For the capacities of the 2×2 and 4×4 RV-MIMO systems, both of them descend slowly with the increase of the alignment range since the larger alignment range means the UCA at the receiver is placed beyond the suitable position with the higher probability. Therefore, the increase of the alignment range has a negative impact on the capacity of the RV-MIMO system. Nevertheless, the capacity of the RV-MIMO system is still higher than that of the MIMO system with the identical numbers of antennas and the identical alignment range since the vortex phase is employed.

For the optimal capacities of the RV-MIMO systems, the capacity of the 4×4 system is fluctuant within a little scope since multiple antennas are placed in a small range $R_{\mathrm{TX}} = 0.8\lambda$, and the antenna correlation could lead to the fluctuation of the capacity. However, the optimal capacity of the 2×2 system keeps a line since less antennas are easier to find the optimal vortex phase. With the identical numbers of antennas and the alignment range, the capacities of the optimal RV-MIMO systems are higher than the RV-MIMO systems since the vortex phase is optimized.

Note that, when the alignment range is 0, the central point of the UCA at the receiver is considered to be fixed. For example, when SNR=8 dB in Fig. 5, the optimal capacity of the 2×2 RV-MIMO system, the capacity of the 2×2 RV-MIMO system and the capacity of the 2×2 MIMO system are 5.74 bps/Hz, 5.437 bps/Hz and 3.768 bps/Hz, respectively. When the alignment range is 0 in Fig. 8, the optimal capacity of the 2×2 RV-MIMO system, the capacity of the 2×2 RV-MIMO system and the capacity of the 2×2 MIMO system are 5.74 bps/Hz, 5.437 bps/Hz and 3.768 bps/Hz, respectively. Since the two groups of data are exactly the same, the results of the Fig. 5 and Fig. 8 are consistent.

Overall, the proposed RV-MIMO system could provide much higher capacity than the MIMO system under the same situation since the vortex phase is exploited. Furthermore, when the central point of the UCA at the receiver is moved and not coincided with that of the UCA at the transmitter, the capacity of the RV-MIMO system decreases slowly. However, the minimum capacity of RV-MIMO system is still higher than that of the MIMO system with the same number of antennas.

VI. DISCUSSIONS

Compared with some related studies [10], [11], [13], the proposed system is different. Firstly, multiple SPPs are employed at the transmitter. Each transmitting antenna is matched to an SPP with different thicknesses to form different vortex signals. Therefore, multiple vortex signals are transmitted simultaneously, and multiple OAM channels are exploited beyond the spatial multiplexing of the MIMO system. There is no effective method to create multiple vortex signals simultaneously in [10], [11], [13], although they can be generated separately. Thus, there is only one vortex signal at any time, and no extra capacity gains are created beyond the MIMO spatial multiplexing. Secondly, the UCAs in the proposed system are the same as those employed in [10]. However, the results are different since different SPPs are employed at the transmitter. In [11] and [13], the concentric array is adopted. The array is different from the UCA in this paper. In a word, multiple vortex signals are generated simultaneously in the proposed RV-MIMO system. Different vortex signals provide different vortex phases which can be employed as degrees of freedom to provide higher capacity than the conventional MIMO system.

VII. CONCLUSION

In this paper, we proposed an RV-MIMO system and modeled the vortex channel of the proposed RV-MIMO system in free space. The proposed RV-MIMO system exploits the vortex phase of the vortex channel matrix to improve the capacity significantly. Moreover, we derived the optimal vortex phase to enhance the capacity of the proposed RV-MIMO system efficiently. Simulation results show that the RV-MIMO system can provide prominent improvements for both the capacity and the optimal capacity compared with the MIMO system in free space.

REFERENCES

[1] A. Al-Dulaimi, S. Al-Rubaye, Q. Ni, and E. Sousa, "5G communications race: Pursuit of more capacity triggers LTE in unlicensed band," *IEEE Veh. Technol. Mag.*, vol. 10, no. 1, pp. 43–51, Mar. 2015.

[2] E. Björnson, J. Hoydis, M. Kountouris, and M. Debbah, "Massive MIMO systems with non-ideal hardware: Energy efficiency, estimation, and capacity limits," *IEEE Trans. Inf. Theory*, vol. 60, no. 11, pp. 7112–7139, Nov. 2014.

[3] W. Nam, D. Bai, J. Lee, and I. Kang, "On the capacity limit of wireless channels under colored scattering," *IEEE Trans. Inf. Theory*, vol. 60, no. 6, pp. 3529–3543, Jun. 2014.

[4] F. Bentosela, N. Marchetti, and H. D. Cornean, "Influence of environment richness on the increase of MIMO capacity with number of antennas," *IEEE Trans. Antennas Propag.*, vol. 62, no. 7, pp. 3786–3796, Jul. 2014.

[5] X. Pu, S. Shao, K. Deng, and Y. Tang, "Analysis of the capacity statistics for 2×2 3D MIMO channels in short-range communications," *IEEE Commun. Lett.*, vol. 19, no. 2, pp. 219–222, Feb. 2015.

[6] F. Tamburini, E. Mari, A. Sponselli, B. Thidé, A. Bianchini, and F. Romanato, "Encoding many channels on the same frequency through radio vorticity: First experimental test," *New J. Phys.*, vol. 14, no. 3, pp. 033001-1–033001-17, Mar. 2012.

[7] Y. Yan *et al.*, "High-capacity millimetre-wave communications with orbital angular momentum multiplexing," *Nature Commun.*, vol. 5, Sep. 2014, Art. ID 4876.

[8] M. Oldoni *et al.*, "Space-division demultiplexing in orbital-angular-momentum-based MIMO radio systems," *IEEE Trans. Antennas Propag.*, vol. 63, no. 10, pp. 4582–4587, Oct. 2015.

[9] M. Tamagnone, J. S. Silva, S. Capdevila, J. R. Mosig, and J. Perruisseau-Carrier, "The orbital angular momentum (OAM) multiplexing controversy: OAM as a subset of MIMO," in *Proc. 9th Eur. Conf. Antennas Propag.*, Apr. 2015, pp. 1–5.

[10] O. Edfors and A. J. Johansson, "Is orbital angular momentum (OAM) based radio communication an unexploited area?" *IEEE Trans. Antennas Propag.*, vol. 60, no. 2, pp. 1126–1131, Feb. 2012.

[11] K. A. Opare and Y. Kuang, "Performance of an ideal wireless orbital angular momentum communication system using multiple-input multiple-output techniques," in *Proc. Int. Conf. Telecommun. Multimedia*, Jul. 2014, pp. 144–149.
[12] K. A. Opare, Y. Kuang, J. J. Kponyo, K. S. Nwizege, and Z. Enzhan, "The degrees of freedom in wireless line-of-sight OAM multiplexing systems using a circular array of receiving antennas," in *Proc. 5th Int. Conf. Adv. Comput. Commun. Technol.*, Feb. 2015, pp. 608–613.
[13] K. A. Opare, Y. Kuang, and J. J. Kponyo, "Mode combination in an ideal wireless OAM-MIMO multiplexing system," *IEEE Wireless Commun. Lett.*, vol. 4, no. 4, pp. 449–452, Aug. 2015.

QIBIAO ZHU received the B.S. and M.S. degrees from the China University of Mining and Technology, Xuzhou, China, in 2003 and 2006, respectively. He is currently pursuing the Ph.D. degree in communications and information systems with the Huazhong University of Science and Technology, Wuhan, China. Since 2006, he has been with the School of Information Engineering, Nanchang University, Nanchang, China. His current research focuses on orbital angular momentum in radio communications.

TAO JIANG (M'06–SM'10) received the B.S. and M.S. degrees in applied geophysics from the China University of Geosciences, Wuhan, China, in 1997 and 2000, respectively, and the Ph.D. degree in information and communication engineering from the Huazhong University of Science and Technology, Wuhan, in 2004. From 2004 to 2007, he was with some universities, such as Brunel University and the University of Michigan–Dearborn, respectively. He is currently a Chair Professor with the School of Electronics Information and Communications, Huazhong University of Science and Technology. He has authored or co-authored over 200 technical papers in major journals and conferences and eight books/chapters in communications and networks. He is a recipient of the NSFC for Distinguished Young Scholars Award in China. He served or serves as a Symposium Technical Program Committee Member of some major IEEE conferences, including INFOCOM, GLOBECOM, and ICC. He was invited to serve as the TPC Symposium Chair of the IEEE GLOBECOM 2013 and IEEE WCNC 2013. He served as an Associate Editor of some technical journals in communications, including the IEEE Transactions on Signal Processing, the IEEE Communications Surveys and Tutorials, the IEEE Transactions on Vehicular Technology, and IEEE Internet of Things Journal.

DAIMING QU received the Ph.D. degree in information and communication engineering from the Huazhong University of Science and Technology, Wuhan, China, in 2003. He is currently a Professor with the Department of Electronics and Information Engineering, Huazhong University of Science and Technology. His current research interests include signal processing, coding, and dynamic spectrum techniques for wireless communications.

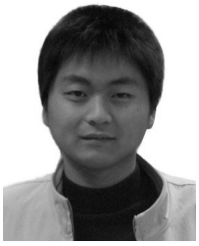

DA CHEN received the B.S. degree in information and communication engineering and the Ph.D. degree from the Huazhong University of Science and Technology, Wuhan, China, in 2009 and 2015, respectively. From 2012 to 2013, he was a Visiting Scholar with Northwestern University, USA. From 2013 to 2014, he was a Visiting Scholar with the University of Delaware, USA. He is currently an Assistant Professor with the School of Electronics Information and Communications, Huazhong University of Science and Technology. His current research interests include various areas in wireless communications, such as Orthogonal Frequency Division Multiplexing and filter bank multicarrier systems.

NANRUN ZHOU received the Ph.D. degree in communication and information systems from Shanghai Jiao Tong University, in 2005. Since 2006, he has served as one of the faculty members of the Department of Electronic Information Engineering with Nanchang University, Nanchang, China, where he is currently a Professor. He is also the Young Scientist of Jiangxi Province (Jinggang Star) and is elected for Ganpo Talent 555 Project, leading a team of researchers carrying out research in communication and information systems. He has authored over 130 papers in refereed international conferences and journals.